Applied Catalysis B: Environmental 189 (2016) 141–150

Contents lists available at ScienceDirect

Applied Catalysis B: Environmental

journal homepage: www.elsevier.com/locate/apcatb

Nanostructured niobium oxyhydroxide dispersed Poly (3-hydroxybutyrate) (PHB) films: Highly efficient photocatalysts for degradation methylene blue dye

Ana P. Heitmann [a], Patrícia S.O. Patrício [b], Italo R. Coura [b], Emerson F. Pedroso [b], Patterson P. Souza [b], Herman S. Mansur [a], Alexandra Mansur [a], Luiz C.A. Oliveira [a,*]

[a] Department of Chemistry, Federal University of Minas Gerais, Av. Antônio Carlos 6627, Campus Pampulha, 31270-901 BH-MG, Brazil
[b] Department of Chemistry, Federal Center of Technological Education of Minas Gerais, CEFET-MG, Av. Amazonas 5253, 30421-169 BH-MG, Brazil

ARTICLE INFO

Article history:
Received 15 October 2015
Received in revised form 19 January 2016
Accepted 12 February 2016
Available online 15 February 2016

Keywords:
Photocatalysis
PHB
Niobium oxyhydroxide

ABSTRACT

In this work, nanostructured niobium oxyhydroxide was dispersed over poly (3-hydroxybutyrate) (PHB), which is a biopolymer, for application as a photocatalyst using visible and UV light. PHB films with different amounts of niobium oxyhydroxide were characterized by diffuse UV–vis reflectance spectroscopy, FTIR-ATR and SEM. The characterizations showed particles of the niobium compound well-dispersed on the polymeric matrix, thus modifying the bandgap value, which improved the photocatalysis process. The material showed excellent catalytic activity (approximately 100% degradation) for the oxidation of methylene blue dye considering the reaction in a continuous flow bath. Moreover, the polymer films were easily removed from the solution after the reaction and reused several times while retaining their high activity. ESI–MS studies showed that the dye removal occurs by the formation of reaction intermediates due to the successive hydroxylation of the dye structure, confirming that the reaction took place improved by photocatalytic conditions.

1. Introduction

Wastewater containing organic pollutants represents one of the main causes of environmental pollution, thus presenting a threat to human health and the ecosystem [1]. After their discharge into the environment, these contaminants present resistance to conventional chemical methods and physical removal [2]. Photocatalytic degradation has attracted great interest as a process for removing organic and inorganic contaminants from wastewater [3–5]. However, the cost and technical barriers involved have hampered the application of photocatalysis because the recovery of the catalyst from the aqueous medium, when possible, is time-consuming and expensive.

Niobium oxides are promising materials for use in various reactions such as hydration, esterification, condensation and heterogeneous photocatalysis in advanced oxidation processes due to their special properties, such as their high BET surface area, high selectivity, and acidic sites [6,7]. Niobium catalysts have been found to be efficient in the oxidation of organic compounds in the aqueous medium and organic photodegradation of pollutants in the presence of ultraviolet radiation or sunlight [8]. Furthermore, the niobium oxides can be combined with other metals, such as platinum, ruthenium and rhodium, to improve their performance in many catalytic processes [9]. With respect to photocatalysis, two questions are considered to be crucial for the proper application of technology on an industrial scale: (i) the radiation-absorbing capacity of the photocatalyst in the visible region and (ii) its recovery for reuse. The recovery of a catalyst with nanometric dimensions from an aqueous medium is a complicated process, and many times the catalyst must be combined with other materials to promote solid/liquid separation. The importance of the immobilization of the catalysts in a matrix or on a support for application in photocatalysis has been growing in recent years, mainly due to their ease of removal from the aqueous medium for reuse [10].

Immobilization may allow the light absorption to be optimized because a polymeric matrix containing the immobilized catalyst can be positioned on the surface of the liquid containing the pollutant to be degraded. In recent years, various polymeric supports for catalysts have been studied because they exhibit high stability in the aqueous medium, have a low cost and are chemically inert [11].

* Corresponding author.
E-mail address: luizoliveira@qui.ufmg.br (L.C.A. Oliveira).

http://dx.doi.org/10.1016/j.apcatb.2016.02.031

Among the studied catalyst-polymer systems reported, the literature highlights that the thin films of polyethylene/TiO_2 (PE/TiO_2) and polypropylene/TiO_2 (PP/TiO_2) used for methylene blue dye degradation in the presence of UV radiation have higher stabilities compared to the commercially available material for the same purpose [12]. The polyethylene terephthalate (PET/TiO_2) system used for oxidation of As (III) to As (V) and removal of As (V) from the aqueous medium in the presence of ferric oxyhydroxide (II) and sunlight presents major advantages such as the use of low cost materials in the process and the removal of 94% of As (V) in natural water in only 60 min [13]. The composite of polyaniline (PANI/TiO_2) used for the degradation of methylene blue in the presence of visible radiation exhibited a high catalytic efficiency, yielding approximately 80% removal of the analyte in only 90 min [14]. Recently, Ghosh et al. [15] presented an interesting study employing a conductive polymer (poly(diphenylbutadiyne) (PDPB)) directly as a photocatalyst for dye degradation in aqueous medium.

However, sophisticated and expensive methods for impregnating the catalyst on the matrix, such as the sol-gel process, *in situ* chemical polymerization, and the spray coating technique, makes the development of these materials expensive. Moreover, all investigated polymers are synthetic with a difficult degradation process when released into the environment. Studies involving renewable polymers and materials have become necessary due particularly to their biodegradability and lower toxicity to the environment [16,17].

In a pioneering work reported by Yew et al. [10] the polymeric system poly (3-hydroxybutyrate) PHB/TiO_2 was studied for the degradation of organic contaminants and antibacterial activity via photocatalytic sterilization. In the study, the authors used a high amount of titanium dioxide in the polymer matrix, approximately 57 wt%. PHB is a biopolymer produced from renewable sources, *i.e.*, from fermentation by certain micro-organisms. In addition to being naturally biodegradable, PHB shows some properties similar to those of synthetic polymers, especially polypropylene [18–20]. Materials with this characteristic are attractive, as they are assimilated and decomposed by microorganisms making them easily converted into simple and mineralized compounds [21].

In this work, we report the development of a new catalytic system based on a PHB polymer film containing up to 5 wt% of highly dispersed niobium oxyhydroxide. The materials were produced via casting with slow evaporation of the solvent. The photocatalytic activity of this material under UV and visible light for the degradation of methylene blue dye was tested. The characteristics of this material permitted the reactions to be tested in a continuous flow system.

2. Experimental

2.1. Materials and chemicals

The oxyhydroxide niobium (S_2) was prepared in accordance with previous work of our group [8]. The catalyst was obtained using $NH_4[NbO(C_2O_4)(H_2O)](H_2O)n$, donated by CBMM—Companhia Brasileira de Metalurgia e Mineração (Araxá, state of Minas Gerais, Brazil), NaOH (Sigma-Aldrich) and H_2O_2 30% v/v (Synth). For the preparation of the nanocomposites were used PHB (ca. 600 kDa) from PHB Industrial S/A. (Serrana-SP-Brazil), chloroform (Synth) and dimethylformamide (Synth).

2.2. Preparation of PHB/S_2 nanocomposite film

The PHB and PHB/S_2 films, shown in Fig. 1, were obtained via the casting technique. For the preparation of the films, PHB powder was solubilized in chloroform and dimethylformamide (DMF) with the addition of oxyhydroxide niobium (S_2) at concentrations of 1, 2, 3 and 5 wt%. The solution was placed under constant agitation and heating to approximately 55 °C for 4 h until complete dissolution was achieved. The mixture was poured into a glass Petri dish and the solvent was left to evaporate at room temperature for 72 h. Then, the samples were dried at 60 °C for 24 h.

2.3. Characterization of the materials

The structural properties of PHB and PHB/S_2 composites were investigated by various characterization techniques. The diffuse reflectance spectra of the materials were obtained using a Shimadzu 3550 UV–vis spectrophotometer coupled with a diffuse reflectance detector listed in the region from 200 to 800 nm. The reflectance data were converted to a reissued function (Eq. (1)) called the Kubelka-Munk function and is defined as:

$F(R) = \frac{(1-R)^2}{2R} = \frac{k}{s}$ (1)where in R is the absolute reflectance, and k is the coefficient of the absorption and s is the coefficient of scattering. The indirect bandgap calculation (Eq. (2)) was determined by the Tauc formalism, which was considered for only direct transitions with n = ½ [22].

$\alpha h\nu^n = (F(R)) \times h\nu^n$(2)

α is the absorption coefficient, h is Planck's constant, and ν is the frequency of the radiation.

The morphologies of the materials were characterized by scanning electron microscopy (SEM) using a JEOL scanning 840A model microscope operated at 7 kV. Chemical mapping was conducted using a Shimadzu model SSX-550 instrument operated at 15 kV. Infrared spectroscopy (FTIR) was realized in a Thermo Scientific spectrophotometer equipped with an attenuated total reflection accessory (micro-crystal ZnSe ATR with 300 mM) using a Cassegrain microscope (Centaurus, 10× magnification) in the reflection mode.

2.4. Catalytic tests

The catalytic tests were performed at 25 °C using 15 mL of methylene blue solution (20 mg L^{-1}) containing 0.5 g of polymer films with a stirring rate of 330 rpm using a mechanical stirrer for 10–120 min. A UV lamp (mercury vapor, λ = 254 nm- TOVALIGHT GLT) and visible radiation (dichroic lamp, λ > 400 nm- TOSCHIBRA) were used. The oxidation efficiency was monitored with a UV–vis

Fig. 1. Image of the PHB/S2 film obtained by casting.

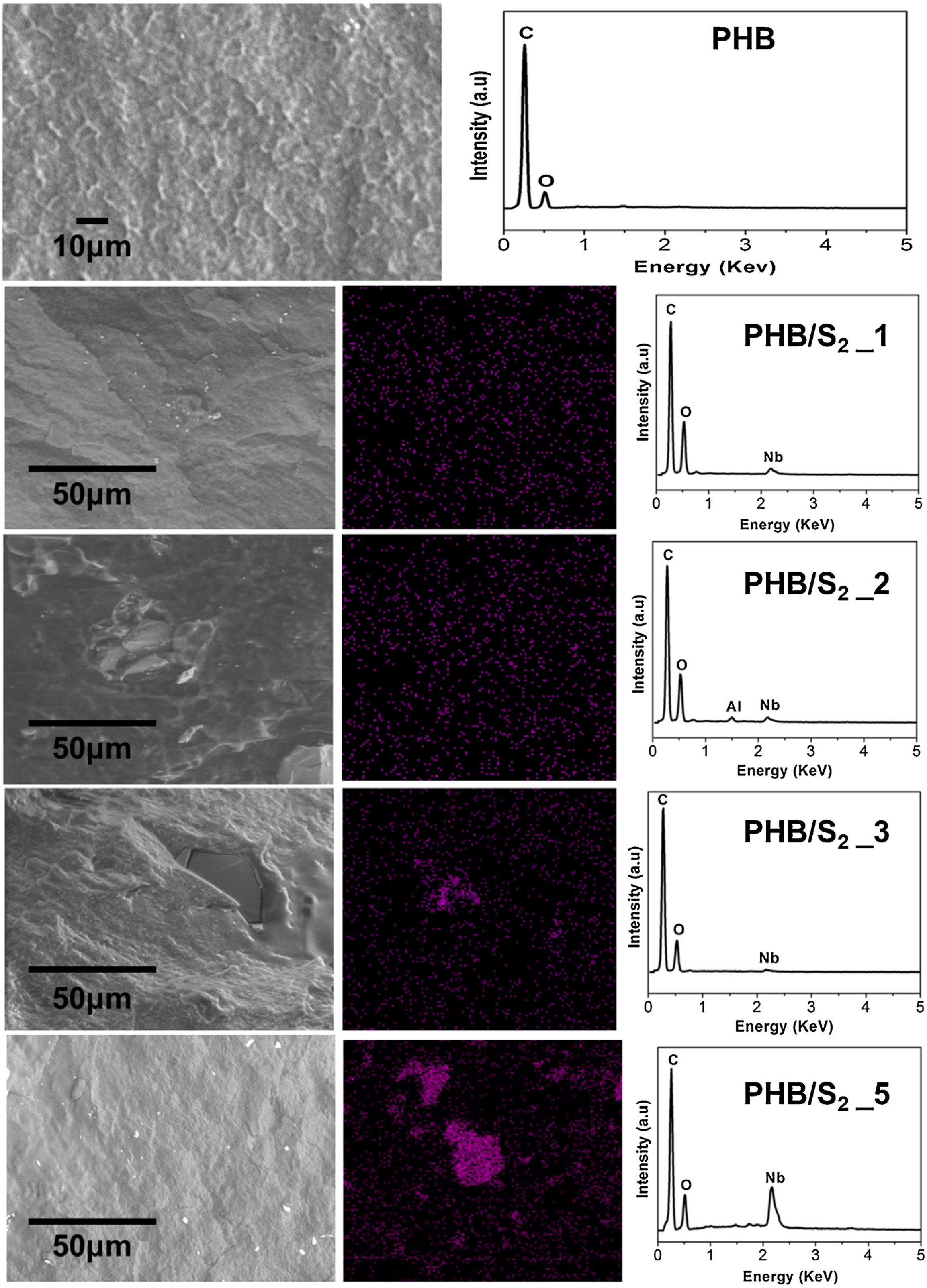

Fig. 2. SEM images: surface of the cryogenic fracture (secondary electron) of the PHB and nanocomposites PHB/S2_1, PHB/S2_2, PHB/S2_3 and PHB/S2_5 (left) and chemical mapping (electron backscattering) of nanocomposites films (middle). The EDS spectra of films (right) obtained focusing on the light regions in the SEM images by secondary electron.

spectrophotometer (Shimadzu, UV-1601 PC) at 664 nm, which is a characteristic wavelength of the methylene blue dye. To identify the intermediate chemical species formed during the oxidation of methylene blue, ESI–MS was used. For the tests in continuous flow, 5 g of polymeric films and 250 mL of methylene blue dye solution (20 mg L^{-1}) were employed. A PVC pipe was used as the photore-

Table 1
Band gaps of nanocompounds PHB/S_2 materials.

Materials	Bandgap value/eV
PHB/S2 _1	2.53
PHB/S2 _2	2.67
PHB/S2 _3	2.91
PHB/S2 _5	2.97
S2	3.00

actor. The PVC pipe was coated with various polymeric films that are flexible for introducing and were easily adhered to the surface of the photocatalyst. We used a peristaltic pump for circulating the dye solution at a flow of 60 L h^{-1}. The system used is shown in supporting information (Fig. S1).

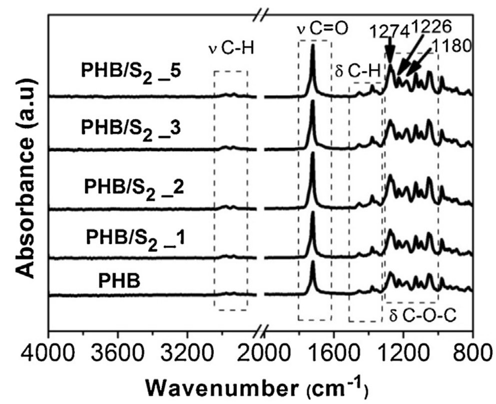

Fig. 3. FTIR-ATR spectra of the PHB film and 1–5 wt% composite PHB/S_2.

3. Results and discussion

3.1. Characterization of the materials

The materials were characterized by diffuse reflectance spectroscopy. The data obtained were converted to the Kubelka-Munk reference function (Eq. (1)) and are represented in Table 1.

S_2 has a bandgap value of 3.0 eV. To the composites containing 1, 2, 3 and 5 wt% niobium oxyhydroxide bandgap values increased with increasing niobium contents. According to Li et al. [23] incorporation into a support material will result in variation of the bandgap. Nevertheless, the bandgaps of PHB/S2 films show lower values than those with niobium oxyhydroxide particles. The composites can be excited to produce electron-hole pairs in the presence of visible and UV light, which can result in a high catalytic activity as reported by Li et al. [23]. The SEM/EDS technique was used to evaluate the morphologies and chemical compositions of the cryogenic fractures of PHB/S2 films (Fig. 2).

The SEM images shown in Fig. 2 correspond to the cryogenic fractures of pure PHB and PHB/S2 composites. The fracture profile is typical of brittle materials and characteristic of PHB. The SEM images show no significant differences in the film fracture patterns because they present similar formations of cracks. In the EDS spectra, focusing on the light regions observed in the sample fracture SEM images, 1–5% PHB/S2 showed a large amount of niobium, as opposed to that observed in the spectra for the dark region of the PHB matrix, similar to the pure PHB spectra (Fig. 2 right). In the EDS spectra of the PHB/S_2_2 was observed the presence of aluminum which may be attributed to some contamination in the preparation of nanocomposites.

It is suggested that the light phases in the SEM images are agglomerates of nanoparticles present in the polymer matrix. The images obtained by SEM and chemical mapping results indicate that good distributions of the agglomerates on the entire polymer matrix for all of the concentrations of niobium oxyhydroxide were obtained [24].

S2 was characterized by FTIR. The profile bands in spectra are typical of niobium oxyhydroxide with vibration about 3100 cm-1 related to bulk hydroxyl group present in this material [25]. This type of vibration is characteristic of an oxyhydroxide phase as described in our previous work [26,27]. Pure PHB and PHB/S_2 composites were investigated using FTIR-ATR (Fig. 3). The FTIR-ATR spectrum of the pure PHB is characterized by the presence of bands between 3000 and 2900 cm^{-1} related to the symmetrical stretching of the CH_3 group as well as bands from 1460 to 1380 cm^{-1} associated with asymmetric stretching and CH_2 groups. The bands that appear in the FTIR-ATR spectrum of PHB can be related to two primary components corresponding to the crystalline and amorphous phases.

The bands in the region of 1300–1100 cm-1 correspond to the symmetric and asymmetric stretching of the COC group. The crystalline phase is associated with bands at 1274 and 1226 cm^{-1}, and the amorphous phase is associated with bands at 1261 and 1180 cm^{-1}. In the spectrum, it is possible to identify bands at 1700–1650 cm^{-1}, which are due to carbonyl stretching vibrations of ester groups of the polymer [28–32].

The spectra of pure PHB and films containing niobium oxyhydroxide have a similar band pattern. The band with a maximum at 1720 cm^{-1} is commonly exploited in the study of intramolecular and intermolecular interactions involving carbonyl groups because they are important in the organization of PHB crystals [33]. To obtain information on specific interactions in the polymer in the presence of inorganic particles, deconvolution of the bands in the carbonyl group region of the PHB was performed. This study was conducted using the Lorentzian function and is shown in Fig. 4. The fitting reveals the presence of three major bands located in the region between 1800 and 1640 cm-1 corresponding to the carbonyl groups of the crystalline and amorphous phases. The shoulder at 1740 cm-1 is associated with the free C=O, and the most intense band at 1722 cm^{-1} is associated with the C=O groups attached in both the crystalline and amorphous phases. The weak absorption band observed at 1686 cm^{-1} region can be assigned to C=O groups involved in interactions associated with the crystalline phase [34,35]. The 1–5 wt% PHB/S2 films did not show significant shifts in the bands at 1722 cm^{-1} and 1740 cm^{-1}. Comparing the PHB/S2 and pure PHB, is possible to identify only a smooth enlargement of these bands in the presence of the niobium compound. However, in the region of 1686 cm-1 significant shifts are observed when the concentration of the niobium compound increases in the polymer. According to Sato et al. [36] this low intensity band is important because it is sensitive to changes in the polymer structure, particularly the crystalline defects caused by chemical interactions among the components of blends and composites.

Films containing 3 and 5 wt% of niobium oxyhydroxide (PHB/S2_3 and PHB/S2_5) showed a shift of the band from 1687 cm-1 to 1676 cm-1 and 1674, respectively. From the similar behavior of the FTIR spectra reported in the literature, Díez-Pascual and Díez-Vicente [37] and Yu et al. [38] suggest that the interaction of PHB with niobium particles occurs by means of hydrogen bonds involving C=O groups from the ester groups of the PHB and —OH groups present in the niobium oxyhydroxide. The oxyhydroxide synthesized niobium was subjected to treatment with hydrogen peroxide as discussed by Oliveira et al. [39] and Esteves et al. [40] generating peroxo groups, which are highly oxidizing, and hydroxy groups on its surface.

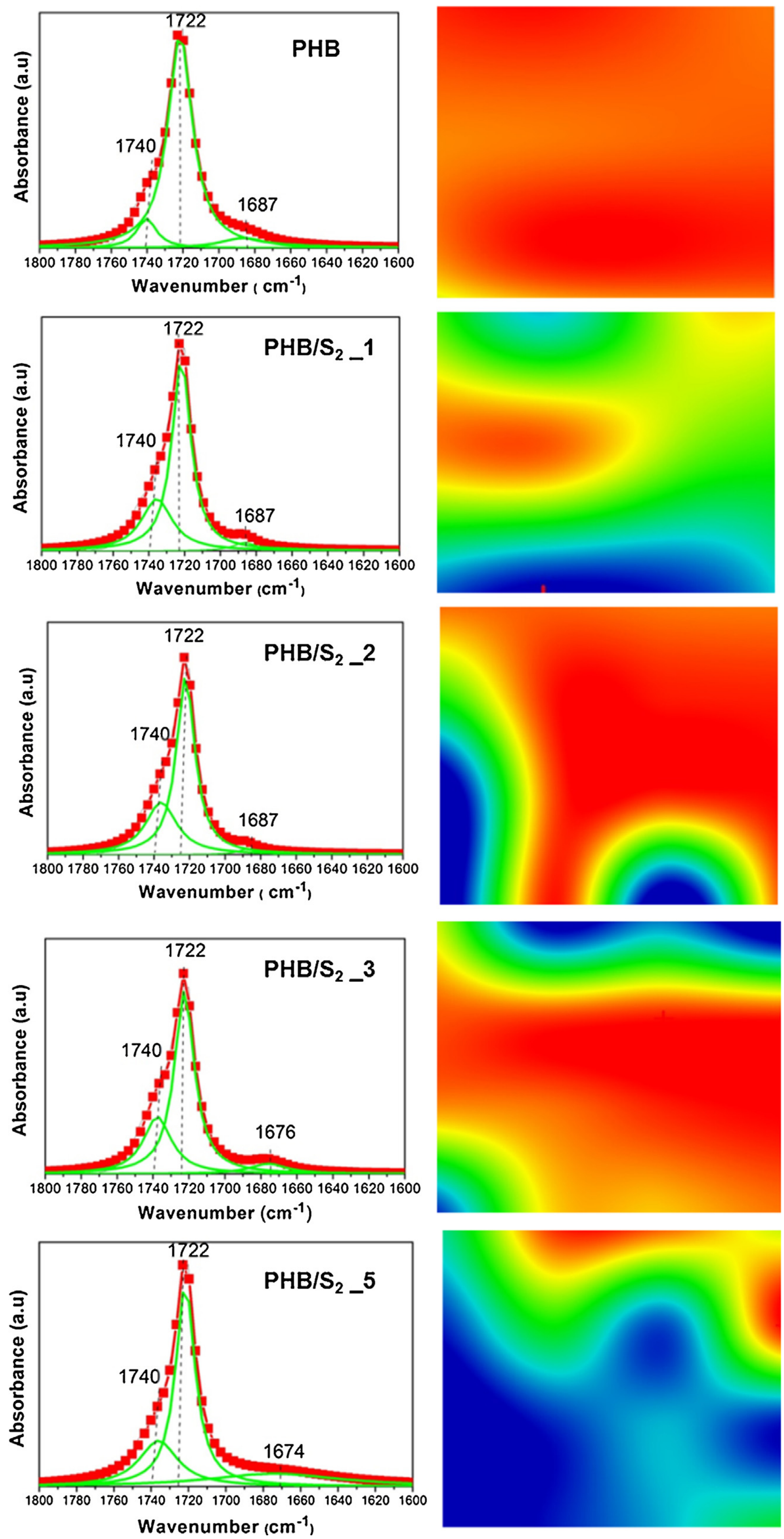

Fig. 4. Lorentzian fit for FTIR-ATR and characteristic curve contour profiles of the carbonyl regions of films of PHB and 1–5 wt% PHB/S2.

The images on the right side of the FTIR spectra in Fig. 4 correspond to the contour profiles of the band displayed in the region between 1800 and 1600 cm^{-1}. For PHB films, there was a single color in the image, showing that the profile of the band did not substantially change along the length of the sample scan. For samples containing PHB and particles of niobium, there is a different behav-

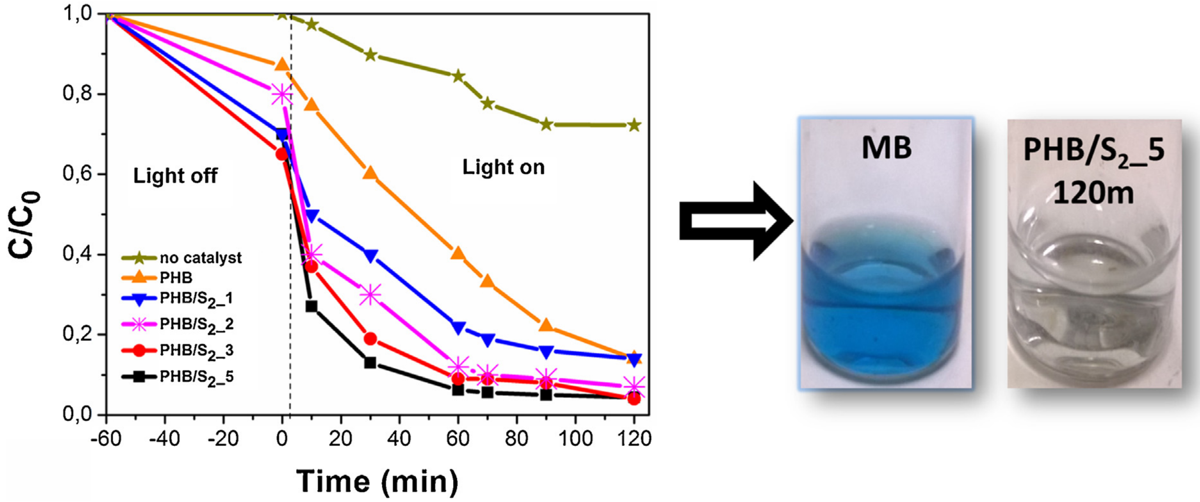

Fig. 5. A profile of the color removal kinetics of a methylene blue dye solution (20 mg L^{-1}) employing the PHB/S2 catalysts.

ior with a strong pattern of changing colors along the length of the sample during scanning to the extent that the concentration of niobium in the film phase increases. The interaction of C=O groups of the polymer with the niobium particles, which are dispersed in the matrix, most likely influenced the band profile, modifying it while scanning. It is believed that as the contribution of the vibrations of groups involved in interactions that occur in the regions of nanoparticle-polymer interface in the absorption band becomes higher, the appearance of other colors is observed.

3.2. Catalytic tests

3.2.1. Photocatalytic tests in the presence of UV radiation

The photodegradation of an aqueous solution of methylene blue in the presence of oxyhydroxide and PHB/niobium composite was monitored by UV–vis spectrometry, and the results are shown in Fig. 5.

When the pure PHB was employed, a low removal capacity by adsorption of the dye was observed, as shown in the profile of Fig. 5 in the absence of light. On the other hand, materials containing niobium oxyhydroxide had better adsorption capacities, and the PHB_5 catalyst showed a removal of approximately 30%. The curve shows that decoloration of the solution occurred only in the presence of UV light without catalytic, about 30% after 90 min (photolysis). In the presence of catalyst and UV light, the color removal of the dye solution was complete after 120 min. After the addition of pure PHB under UV light, the discoloration increased, this indicated that another process runs in addition to the photolysis. Probably this process is related to the formation of hydroxyl radicals, which are generally formed from the surface degradation of PHB in the presence of oxygen, humidity and UV radiation [41].

The composites that have oxyhydroxide niobium in their constitution revealed high catalytic activities compared to pure polymer. In fact, the materials containing 3–5 wt% of niobium oxyhydroxide showed complete removal of color after only 30 min of reaction time. The semiconductor niobium oxyhydroxide has a bandgap of 3.0 eV, as discussed earlier, which displays a good catalytic activity. Nogueira et al. [42] reported similar results using only the niobium oxyhydroxide after treatment with hydrogen peroxide. However, the use of finely powdered material without deposition over a polymeric matrix did not allow its recovery for reuse. Furthermore, the PHB/S2 composite showed a higher catalytic efficiency than SnO2 thin films which bandgap (3.6 eV) is higher than of niobium oxyhydroxide (3.0 eV) [40] and higher than nanotube titanium dioxide, a widely studied material for photocatalysis that

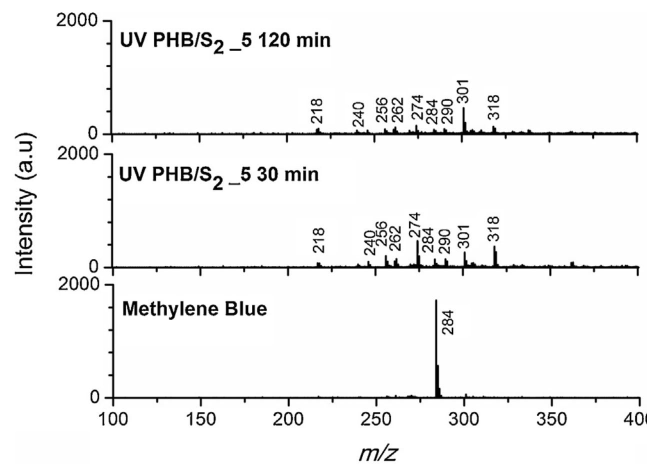

Fig. 6. ESI(+)-MS methylene blue solution before and after 30 and 120 min of reaction time using photocatalysis with the PHB/S2_5 catalyst under UV radiation.

showed 79% removal of methylene blue in an aqueous medium using UV radiation [43].

While the materials presented in this work have shown high dye removal capacities, the study via UV–vis spectroscopy proves the effective degradation of the organic molecule. Thus, the degradation of methylene blue by niobium catalysts incorporated into PHB was monitored by ESI(+)-MS to identify photocatalysis intermediates (Fig. 6). The study was conducted after 30 and 120 min of reaction time. Due to its higher removal efficiency, the resulting reaction solution using the PHB/S_2_5 material was studied. The spectrum of the dye indicates the presence of a single peak at $m/z = 284$ that is characteristic of the methylene blue aqueous solution [44].

After reaction, the characteristic peak intensity of the dye decreases significantly, and other peaks associated with the intermediaries appear. Concurrently with the decrease of the $m/z = 284$ signal, there is the emergence of various ions ($m/z = 301$, 318, 338, 218, 262 and 256), suggesting the occurrence of the oxidation and demethylation reactions of dye molecules [43]. The peaks at $m/z = 256$ and $m/z = 274$ refer to the beginning of the degradation of the organic molecule indicating the demethylation of methylene blue. The signals $m/z = 218$, 240 and other signals with a lower mass than methylene blue are evidence that the structure of the molecule was degraded, which shows an advanced stage of oxidation before

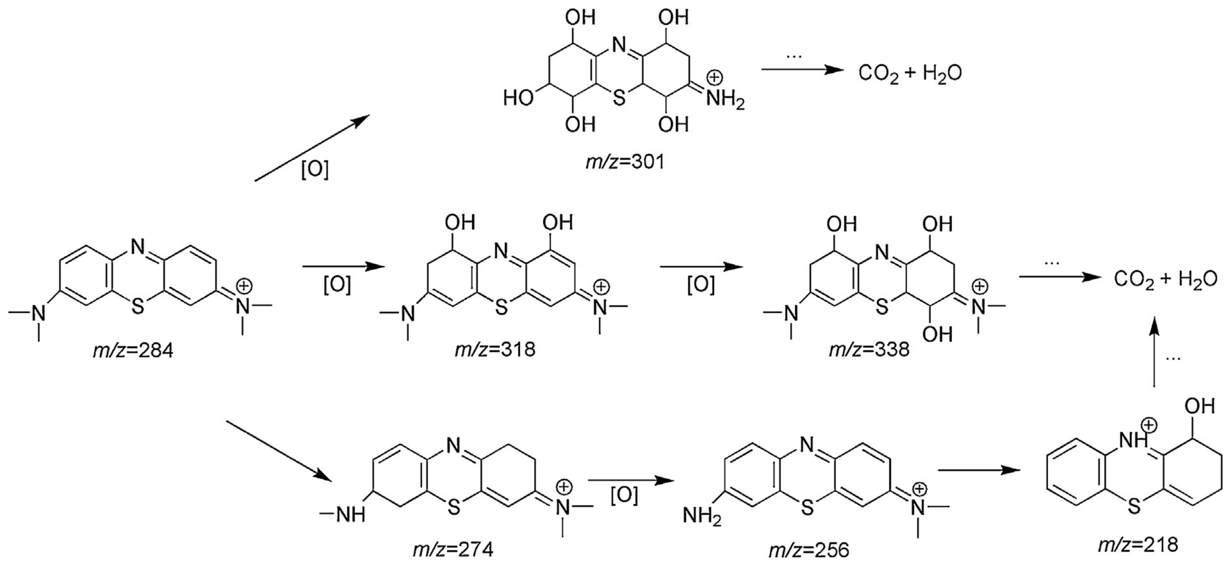

Fig. 7. Proposal of the main intermediaries involved in the degradation of methylene blue.

mineralization [45]. Furthermore, the signals at $m/z = 301$, $m/z = 318$ and $m/z = 338$ suggest successive hydroxylations, indicating that the HO$^\bullet$ radicals generated *in situ* by the photocatalytic process are incorporated into the dye structure promoting its oxidation [27,46,47]. It is interesting to note that with only 30 min of reaction time, it is possible to identify a large proportion of ions corresponding to significant dye degradation with a decreasing signal at a $m/z = 284$ concerning the dye. The spectrum of the solution obtained after 120 min of reaction shows the signals referring to the same intermediates but with less intensity, indicating that there was degradation of these compounds, possibly via mineralization. The occurrence of other peaks associated with intermediate species after the reaction shows that the degradation of the dye occurs instead of only the adsorption process.

The structures of the intermediates are proposed in Fig. 7.

Yew et al. [10] conducted a similar study to the one presented here, where a PHB polymer matrix was employed for the dispersion of TiO_2 semiconductor. The authors succeeded in removing 96% of the methylene blue dye. However, higher catalyst concentrations were used in the polymer (57% TiO2) compared to in this work as well as a lower concentration of methylene blue. In addition, there was no evidence that the dye was in fact degraded because studies showed no evidence of reaction intermediates as presented via ESI–MS in this study.

The particles of niobium oxyhydroxide after treatment with hydrogen peroxide have been the subject of several studies of our research group, in which the high removal capacity of organic compounds in solution was demonstrated [48]. In the studies, it became apparent that the surface is formed from modified niobium forming "peroxo" groups, which are highly oxidizing. Such oxidizing species can be transferred to the organic compounds in solution, causing their effective oxidation [49]. Additionally, because it is a semiconductor, highly oxidizing hydroxyl radicals can be generated *in situ* by the action of visible or UV radiation. The matrix PHB, due to its hydrophobicity, showed a high stability in the aqueous medium in the presence of visible and UV radiation. With the immobilization of the catalyst to niobium in the polymer matrix, its removal from the aqueous medium has become easier, thus eliminating the costly filtration or centrifugation step and allowing it to be reused for several photocatalytic cycles. To evaluate the stability of the catalyst, the composite showing the best efficiency in the photocatalytic process, PHB/S2_5, was reused for seven successive cycles of 120 min as shown in Fig. 7. To evaluate the stability of the catalyst, the composite showing the best efficiency in the photocatalytic process, PHB/S2_5, was reused for seven successive cycles of 120 min, as shown in Fig. 8.

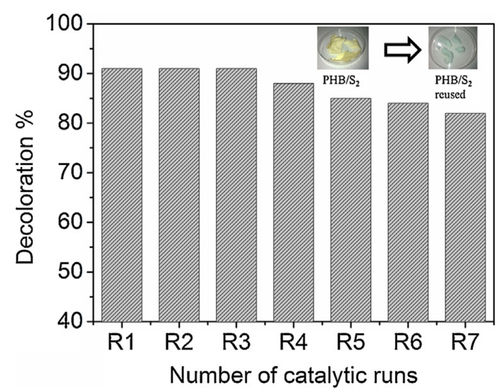

Fig. 8. Color removal of a methylene blue solution (20 mg L^{-1}) after successive reuse of a PHB/S2_5 catalyst.

The catalytic activity was maintained for seven reuses and showed a high removal efficiency of approximately 90% for all of the tests. After being reused, the modified films were a noticeably blue color, most likely due to the adsorption of methylene blue solution, which can be a cause of the partial loss of activity throughout the reuses. SEM images of the PHB/S2_5 catalyst (Fig. 9) after the seventh reuse show the presence of niobium oxyhydroxide, which is mainly present on the surface of PHB, justifying the maintenance of its activity after several reuses.

The EDS spectra obtained for the PHB/S2_5 material before the reaction (Fig. 3) and after seven reuse cycles (Fig. 9) are similar. Comparing the images of the surface and fracture of PHB/S2_5, it is observed that the niobium compound clusters are distributed throughout the material suggesting that there is the preferential accumulation of the niobium oxyhydroxide phase on the surface film and that there is no leaching of the active phase after successive reuses. Furthermore, the recovery of the niobium particles from the PHB matrix becomes possible by solubilization, making this polymer interesting as a substrate for photocatalysis and giving it a great advantage over other materials studied.

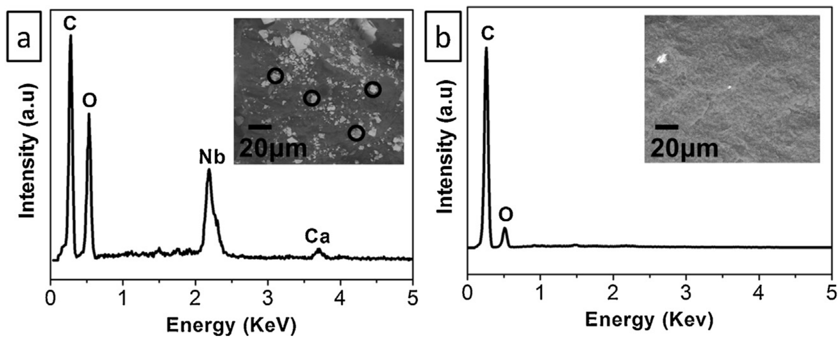

Fig. 9. SEM images/EDS of PHB/S2_5 after seven reuses: (a) surface and (b) fracture.

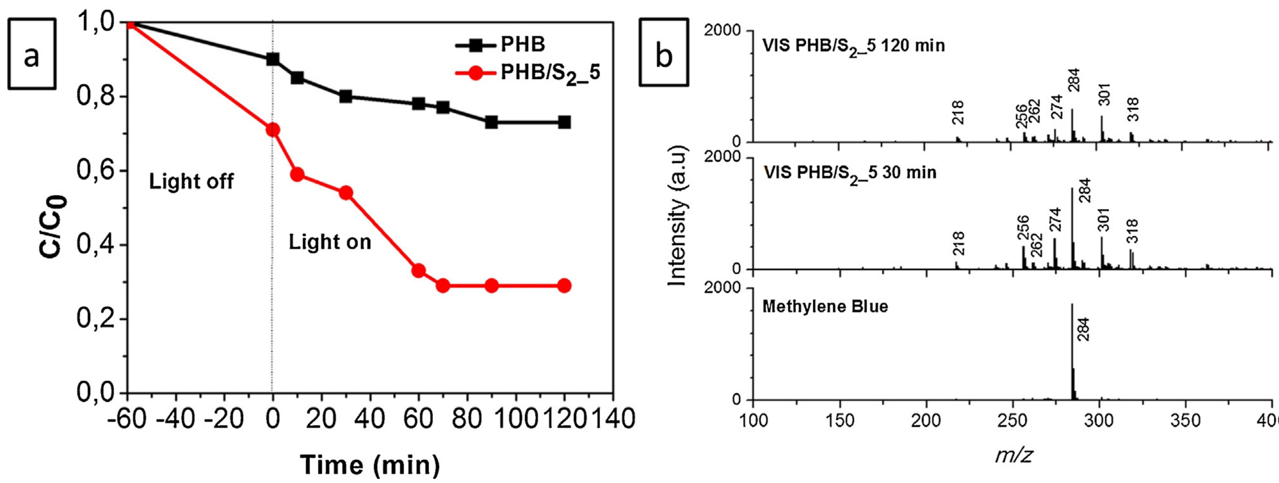

Fig. 10. Profile of methylene blue dye removal (20 mg L^{-1}) employing the pure PHB and PHB/S2_5 catalysts (a), and the ESI–MS signals of the intermediates after 30 and 120 min of reaction time (b).

3.2.2. Photocatalytic tests in the presence of UV–vis irradiation

The material with the best catalytic activity has been tested for the removal of methylene blue using photocatalysis under the action of visible light. This test can indicate the potential of the material to be applied using solar radiation, which would make the process less onerous in the case of use on an industrial scale. Fig. 10a shows the profile of the color removal kinetics comparing the pure PHB and PHB/S2_5 catalysts. The pure PHB showed the ability to remove approximately 25% of the dye from the aqueous medium. The presence of niobium oxyhydroxide in the polymer matrix of the dye significantly improves the removal capacity, removing approximately 70% of the coloring. Again, this process was studied through the formation of intermediates by ESI–MS (Fig. 10b).

After 30 min of reaction time, peaks relating to successive hydroxylations of the dye molecule were observed, indicating the action of $OH^{\bullet}$ radicals from the photocatalytic process. After 120 min of reaction time, the signal m/z = 284 referring to the dye decreases sharply with increasing intensities of signals relating to reaction intermediates. This result indicates that visible light can generate electron-hole pairs promoting the generation of the hydroxyl radical, which is capable of oxidizing organic molecules. The catalytic effect of the presence of visible light is less effective when compared to UV light, but the use of sunlight has been shown to be quite promising.

3.2.3. Photocatalytic tests in continuous flow

A continuous flow test has been conducted to obtain an applied photocatalytic system for the degradation of methylene blue molecules using UV radiation. The measurement of the color removal was obtained continuously every 10 min of reaction time with a UV–vis spectrometer using the determined wavelength of 664 cm^{-1}.The efficiency of the photocatalysis is shown in Fig. 11.

In the flow reactor, methylene blue decoloration in the absence of catalyst under UV radiation was not significant. When the catalyst system employed PHB/S2_5, maximum removal due to photocatalysis remained approximately 90%, similar to the decoloration batch process, whose removal rate reached 96%. The decoloration balance of the photocatalytic process was reached after 300 min. The formation of intermediates was studied by ESI–MS after 530 min of reaction time, and the results are shown in Fig. 11. The intermediates formed during a reaction indicated that the bleaching process should occur effectively by means of photocatalysis. In the continuous flow system, the mechanism has been identified largely from intermediates that are also present in the batch process suggesting that the photocatalysis occurs by the same proposed mechanism forming the structures depicted in Fig. 7.

Mathews [50] used a borosilicate continuous flow system coated with sand impregnated with TiO2, and a 70% removal of methylene blue in the presence of UV radiation was observed. Recently, McCullagh et al. [51] reported the complete degradation of methylene blue using 90–120 g of TiO2 pellets as a catalyst, and Han et al. [52] used glass substrate covered with ZnO nanowires and UV radiation to reach a maximum methylene blue removal of 96%.

This study proposes a system for continuous flow whose polymer film containing the catalyst can be easily removed from the aqueous medium and reused. It is not necessary to use separation methods such as centrifugation or hydrocyclone to separate the catalyst from the aqueous medium making it difficult to reuse as was seen in the studies. Furthermore, the amount of catalyst used is greatly reduced. The efficient polymer/catalyst photocat-

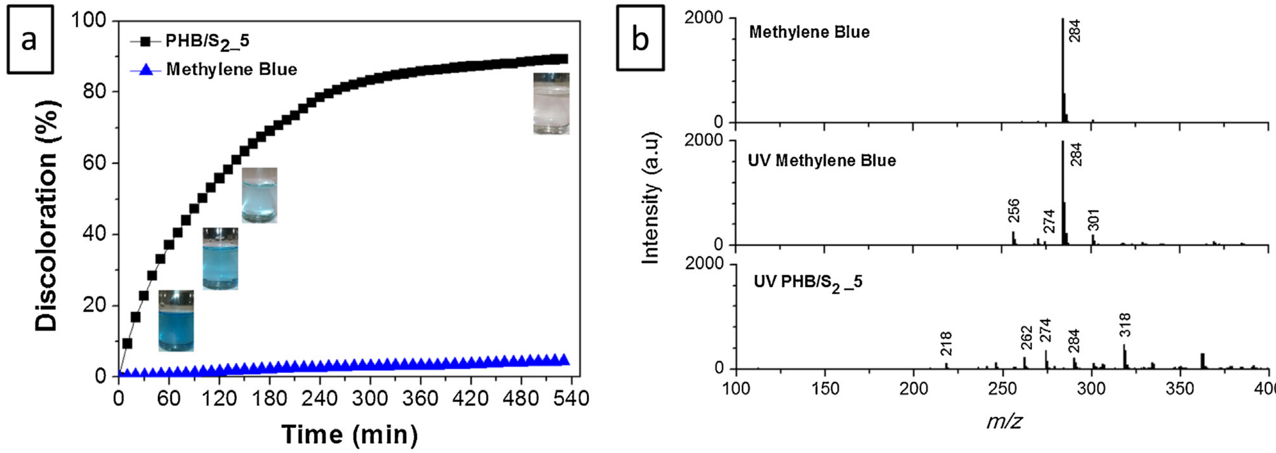

Fig. 11. A profile of the color removal kinetics of a methylene blue dye solution (20 mg L^{-1}) employing the PHB/S2_5 catalyst in continuous flow (a), and the ESI–MS signals of the intermediate after 530 min of reaction time (b).

alytic system presents with a potential application in the treatment of colored industrial wastewater.

4. Conclusions

In this work, a catalyst based on dispersed niobium oxyhydroxide in a biodegradable polymeric matrix (PHB) was developed for the first time. The formed composite proved to be highly efficient for the removal of an organic dye from the aqueous medium in the presence of UV or visible radiation via photocatalysis. SEM analysis suggests that the particles of niobium oxyhydroxide are finely agglomerated and highly distributed throughout the bulk PHB.

The PHB film modified with catalyst remained stable, indicating a slight decrease in color removal after being reused for seven cycles. The photocatalytic tests in continuous flow showed a high catalytic activity using the compound PHB/S2, which was easily recovered from the aqueous solution after the photocatalysis steps without requiring filtration or centrifugation. Finally, the ESI–MS study showed an enhanced dye oxidation stage, indicating that in fact the degradation of the organic dye occurs.

Acknowledgments

This work was supported by grants from CNPq, FAPEMIG and CAPES.

Appendix A. Supplementary data

Supplementary data associated with this article can be found, in the online version, at http://dx.doi.org/10.1016/j.apcatb.2016.02.031.

References

[1] I.K. Konstantinou, T.A. Albanis, Appl. Catal. B Environ. 49 (2004) 1–14.
[2] M.M. Khin, A.S. Nair, V.J. Babu, R. Murugan, S. Ramakrishna, Energy Environ. Sci. 5 (2012) 8075–8109.
[3] P. Chagas, H.S. Oliveira, R. Mambrini, M. Le Hyaric, M.V. De Almeida, L.C.A. Oliveira, Appl. Catal. A Gen. 454 (2013) 88–92.
[4] Z. Liu, Y.E. Miao, M. Liu, Q. Ding, W.W. Tjiu, X. Cui, T. Liu, J. Colloid Interface Sci. 424 (2014) 49–55.
[5] J.D. Torres, E. a. Faria, J.R. SouzaDe, A.G.S. Prado, J. Photochem. Photobiol. A Chem. 182 (2006) 202–206.
[6] O.F. Lopes, E.C. Paris, C. Ribeiro, Appl. Catal. B Environ. 144 (2014) 800–808.
[7] M. Zarei-Chaleshtori, M. Hosseini, R. Edalatpour, S.M.S. Masud, R.R. Chianelli, Microchem. J. 110 (2013) 361–368.
[8] L.C.A. Oliveira, M. Gonçalves, M.C. Guerreiro, T.C. Ramalho, J.D. Fabris, M.C. Pereira, K. Sapag, Appl. Catal. A Gen. 316 (2007) 117–124.
[9] J.C. Rooke, T. Barakat, J. Brunet, Y. Li, M.F. Finol, J.F. Lamonier, J.M. Giraudon, R. Cousin, S. Siffert, B.L. Su, Appl. Catal. B Environ. 162 (2015) 300–309.
[10] S.P. Yew, H.Y. Tang, K. Sudesh, Polym. Degrad. Stab. 91 (2006) 1800–1807.
[11] G.F. Shan, X. Gong, W.P. Chen, L. Chen, M.F. Zhu, Colloid Polym. Sci. 289 (2011) 1005–1014.
[12] J.H. Yang, Y.S. Han, J.H. Choy, Thin Solid Films 495 (2006) 266–271.
[13] A.H. Fostier, M.D.S.S. Pereira, S. Rath, J.R. Guimarães, Chemosphere 72 (2008) 319–324.
[14] F. Wang, S.X. Min, Chinese Chem. Lett. 18 (2007) 1273–1277.
[15] S. Ghosh, N.A. Kouamé, L. Ramos, S. Remita, A. Dazzi, A. Deniset-Besseau, P. Beaunier, F. Goubard, P.H. Aubert, H. Remita, Nat. Mater. (2015) 1–7.
[16] A. Mohamed El-Hadi, Polym. Bull. 71 (2014) 1449–1470.
[17] G. Burlein, M. Rocha, Mater. Res. 17 (2014) 203–212.
[18] M.P. Arrieta, E. Fortunati, F. Dominici, E. Rayón, J. López, J.M. Kenny, Polym. Degrad. Stab. 107 (2014) 139–149.
[19] A. Sathish, K. Glaittli, R.C. Sims, C.D. Miller, J. Polym. Environ. 22 (2014) 272–277.
[20] M.J. Fabra, A. Lopez-Rubio, J.M. Lagaron, J. Food Eng. 127 (2014) 1–9.
[21] M. Naffakh, C. Marco, G. Ellis, S.R. Cohen, A. Laikhtman, L. Rapoport, A. Zak, Mater. Chem. Phys. 147 (2014) 273–284.
[22] A. Murphy, Sol. Energy Mater. Sol. Cells. 91 (2007) 1326–1337.
[23] X. Li, D. Wang, G. Cheng, Q. Luo, J. An, Y. Wang, Appl. Catal. B Environ. 81 (2008) 267–273.
[24] P.S.D.O. Patrício, F.V. Pereira, M.C. Dos Santos, P.P. De Souza, J.P.B. Roa, R.L. Orefice, J. Appl. Polym. Sci. 127 (2013) 3613–3621.
[25] L.C.A. Oliveira, M.F. Portilho, A.C. Silva, H.A. Taroco, P.P. Souza, Appl. Catal. B Environ. 117-118 (2012) 29–35.
[26] R.M. Cornell, U. Schwertmann, The Iron Oxides, 2nd. ed., J. Willey-VCH, New York, 2003.
[27] L.C.A. de Oliveira, N.T. Costa, J.R. Pliego, A.C. Silva, P.P. de Souza, P.S. Patrícia, Appl. Catal. B Environ. 147 (2014) 43–48.
[28] A. Salehabadi, M.A. Bakar, N.H.H.A. Bakar, Materials (Basel) 7 (2014) 4508–4523.
[29] C.P. Liau, M. Bin Ahmad, K. Shameli, W. Zin, W. Yunus, N.A. Ibrahim, N. Zainuddin, Y.Y. Then, Sci. World J. 2014 (2014) 1–9.
[30] H.S. Barud, J.L. Souza, D.B. Santos, M.S. Crespi, C.A. Ribeiro, Y. Messaddeq, S.J.L. Ribeiro, Carbohydr. Polym. 83 (2011) 1279–1284.
[31] Y.T. Ong, A.L. Ahmad, S.H.S. Zein, K. Sudesh, S.H. Tan, Sep. Purif. Technol. 76 (2011) 419–427.
[32] G.R. Saad, H.E. Salama, N.A. Mohamed, M.W. Sabaa, J. Appl. Polym. Sci. 131 (2014) 9395–9407.
[33] J.P.B. Roa, P.S.D.O. Patrício, R.L. Oréfice, R.M. Lago, J. Appl. Polym. Sci. 128 (2013) 3019–3025.
[34] T. Furukawa, H. Sato, R. Murakami, J. Zhang, Y.X. Duan, I. Noda, S. Ochiai, Y. Ozaki, Macromolecules 38 (2005) 6445–6454.
[35] H. Sato, Y. Ando, J. Dybal, T. Iwata, I. Noda, Y. Ozaki, Macromolecules 41 (2008) 4305–4312.
[36] H. Sato, R. Murakami, A. Padermshoke, Macromolecules 37 (2004) 7203–7213.
[37] A.M. Díez-Pascual, A.L. Díez-Vicente, Int. J. Mol. Sci. 15 (2014) 10950–10973.
[38] Q. Yu, J. Xu, J. Liu, B. Li, Y. Liu, Y. Han, Appl. Surf. Sci. 263 (2012) 532–535.
[39] L.C.A. Oliveira, H.S. Oliveira, G. Mayrink, H.S. Mansur, A.A.P. Mansur, R.L. Moreira, Appl. Catal. B Environ. 152–153 (2014) 403–412.
[40] A. Esteves, L.C.A. Oliveira, T.C. Ramalho, M. Goncalves, A.S. Anastacio, H.W.P. Carvalho, Catal. Commun. 10 (2008) 330–332.
[41] B. Singh, N. Sharma, Polym. Degrad. Stab. 93 (2008) 561–584.
[42] A.E. Nogueira, T.C. Ramalho, L.C.A. Oliveira, Top. Catal. 54 (2011) 270–276.
[43] J. Khan, S.E. Harton, P. Akcora, B.C. Benicewicz, S.K. Kumar, Macromolecules 42 (2009) 5741–5744.

[44] I.S.X. Pinto, P.H.V.V. Pacheco, J.V. Coelho, E. Lorençon, J.D. Ardisson, J.D. Fabris, P.P. Souza, K.W.H. Krambrock, L.C.A. Oliveira, M.C. Pereira, Appl. Catal. B Environ. 119–120 (2012) 175–182.
[45] C.S. Castro, M.C. Guerreiro, L.C.A. Oliveira, M. Gonçalves, A.S. Anastácio, M. Nazzarro, Appl. Catal. A Gen. 367 (2009) 53–58.
[46] W.F. de Souza, I.R. Guimarães, M.C. Guerreiro, L.C.A. Oliveira, Appl. Catal. A Gen. 360 (2009) 205–209.
[47] M.C. Pereira, F.S. Coelho, C.C. Nascentes, J.D. Fabris, M.H. Araújo, K. Sapag, L.C.A. Oliveira, R.M. Lago, Chemosphere 81 (2010) 7–12.
[48] A.C. Silva, R.M. Cepera, M.C. Pereira, D.Q. Lima, J.D. Fabris, L.C.A. Oliveira, Appl. Catal. B Environ. 107 (2011) 237–244.
[49] H.S. Oliveira, L.D. Almeida, V.A.A. De Freitas, F.C.C. Moura, P.P. Souza, L.C.A. Oliveira, Catal. Today 240 (2015) 176–181.
[50] R.W. Matthews, Water Res. 25 (1991) 1169–1176.
[51] C. McCullagh, P.K.J. Robertson, M. Adams, P.M. Pollard, A. Mohammed, J. Photochem. Photobiol. A Chem. 211 (2010) 42–46.
[52] Z. Han, J. Li, W. He, S. Li, Z. Li, J. Chu, Y. Chen, Microelectron. Eng. 111 (2013) 199–203.